
Why In-Context Learning Transformers are Tabular Data Classifiers

Felix den Breejen

KAIST AI

felixdenbreejen@kaist.ac.kr

Sangmin Bae

KAIST AI

bsmn0223@kaist.ac.kr

Stephen Cha

KAIST AI

jooncha@kaist.ac.kr

Se-Young Yun

KAIST AI

yunseyoung@kaist.ac.kr

Abstract

The recently introduced TabPFN pretrains an In-Context Learning (ICL) transformer on synthetic data to perform tabular data classification. As synthetic data does not share features or labels with real-world data, the underlying mechanism that contributes to the success of this method remains unclear. This study provides an explanation by demonstrating that ICL-transformers acquire the ability to create complex decision boundaries during pretraining. To validate our claim, we develop a novel forest dataset generator which creates datasets that are unrealistic, but have complex decision boundaries. Our experiments confirm the effectiveness of ICL-transformers pretrained on this data. Furthermore, we create TabForestPFN, the ICL-transformer pretrained on both the original TabPFN synthetic dataset generator and our forest dataset generator. By fine-tuning this model, we reach the current state-of-the-art on tabular data classification. Code is available at <https://github.com/FelixdenBreejen/TabForestPFN>.

1 Introduction

Tabular data classification is widespread across all industries, leading to an increased interest in the research field of deep learning for tabular data [28, 52, 25, 35]. This type of classification involves classifying a target variable based on a set of attributes, which is commonly stored in tabular format. Examples of tabular classification include predicting the existence of chronic kidney disease based on blood test results [34], estimating the click-through rate of advertisements [38], and predicting the stability of pillars in hard rock mines [29]. Despite the significance of tabular data, major breakthroughs in AI as shown on vision [16, 19, 9] and language [48, 3] data have yet to reach the tabular domain. In fact, neural networks are currently outperformed by tree-based machine learning algorithms such as XGBoost [6] and CatBoost [37] in tabular classification tasks [12, 15, 32].

In an attempt to bridge this performance gap, a recent method called *tabular prior-data fitted networks* (TabPFN) [20] introduces an *in-context learning* (ICL) [8] scheme, demonstrating promising results [15]. This tabular ICL-transformer can predict test observations with only one forward pass using training observations included in the context. Hollmann et al. [20] generate their pretraining data synthetically, with a focus on creating realistic datasets that act as a “prior”. They make their datasets realistic by carefully crafting correlations between features, introducing variety in the feature importance, and by leveraging structural causal models, which can simulate causal relationships.

Even with realistic datasets, it is questionable why pretraining ICL-transformers would improve classification performance on real-world tabular benchmarks. While pretraining in vision and language has clear purposes by transferring texture and grammar knowledge, explanations from a

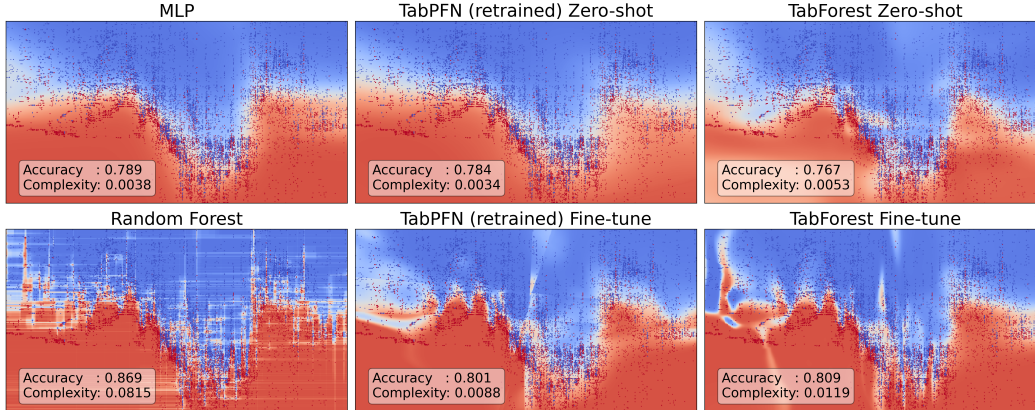


Figure 1: Comparison of decision boundaries for the Electricity dataset (OpenML ID 44156). Axis represent features, colors are predicted class probabilities, and dots are test observations. Fine-tuned variants show a higher complexity score (see section 5.4) than non-fine-tuned variants (Zero-shot).

transfer learning point of view in the field of tabular data do not make sense, as datasets do not share features or labels.

In this work, we claim that the effectiveness of ICL-transformers stems from their ability to form complex decision boundaries. See Figure 1 for an example of such a decision boundary. Intuitively, the complexity is given by how far the decision boundary differs from a simple linear line. Neural networks that train from scratch on tabular data often have overly simple decision boundaries, a phenomenon known as simplicity bias [41], while tree-based methods do not suffer from this [15]. We show that ICL-transformers, in contrast, learn how to create these complex decision boundaries during pretraining. To support our claim, we present three arguments:

- ICL-transformers trained on a highly complex but unrealistic dataset generator achieve performance similar to TabPFN. We create this novel *forest* dataset generator based on decision trees, and we call the ICL-transformer pretrained on this data *TabForest*. Although the generator outputs orthogonal decision boundaries and independent and identically distributed features, the performance of TabForest on individual benchmark datasets is strikingly similar to TabPFN.
- Pretraining dataset complexity is highly correlated with performance. To show this, we vary the parameters of our forest dataset generator that influence the complexity of the decision boundaries. We observe that higher complexity increases the performance.
- ICL-transformers can create decision boundaries with high complexity. This property emerges when fine-tuning on a specific dataset, as illustrated in Figure 1. Furthermore, we observe that complexity increases with the size of the model.

In addition to explaining why ICL-transformers work, we push their performance to new heights. TabForestPFN, the ICL-transformer trained on both the TabPFN and the forest dataset, reaches state of the art on two benchmarks [15, 32]. This ensemble boosts performance by seemingly selecting the best method between TabPFN and TabForest, leveraging the small unexplained differences in performance across various real-world datasets.

We achieve a second major push in performance by switching from *zero-shot* to fine-tuning. The additional fine-tuning phase improves performance on average, even when the number of observations is less than a thousand. Moreover, both fine-tuning and zero-shot performance highly depends on the context size, where larger contexts yield better results, even far beyond the context size pretrained on. These findings suggest that fine-tuning, using the largest possible context size, should be the default choice when working with ICL-transformers.

In conclusion, ICL-transformers are highly effective tabular data classifiers, capable of creating complex decision boundaries. This new insight advances our understanding of tabular ICL-transformers and opens up new avenues for further research to enhance their performance. With further developments, we anticipate a significant shift in the field of tabular data, moving from tree-based methods towards ICL-transformers.

2 Related Works

There are three main branches of tools for tabular data classification: classical statistical methods like linear regression, K-nearest neighbors, and support vector machines [17]; tree-based algorithms like XGBoost [6], CatBoost [37], and LightGBM [24]; and neural-network based methods like this paper. There are several papers benchmarking the different methods [12, 43, 15, 32, 50]. Overall, tree-based methods stand at the top, with neural networks ranging from inferior to at best competitive.

Nonetheless, there have been numerous approaches that tackle tabular data classification with neural networks. First, we have the class of neural networks trained *from scratch*: training starts from random initialized weights and is only trained on the data at hand. Research has focused on architectures [23, 44, 1, 14, 21, 4], embeddings [39, 13, 5], and regularization [42, 22].

In general, methods training from scratch can struggle because tabular datasets can be small. So, researchers have sought ways to use large volumes of tabular data or to change the training objective. Some employ self-supervised learning [26, 49, 54, 2, 46, 45], or closely related transfer learning techniques [33, 27, 53]. Others leverage pretrained LLMs [18, 51] to come to their prediction.

One of those related transfer learning methodologies is *in-context learning*, a new field sparked by TabPFN [20]. Currently, there is ongoing research on how to scale TabPFN to encompass more observations and features [30, 10, 11]. Amid these developments, we present our work.

3 Preliminaries

In tabular classification, we are interested in predicting targets $y \in \mathbb{N}$ given features $x \in \mathbb{R}^d$, where d is the number of features. We predict y using an *in-context learning* (ICL) transformer pretrained on a synthetic dataset. The in-context learning allows the transformer to predict targets based on other observations included in the forward pass. In our work, *zero-shot* refers to one forward pass through the ICL-transformer without any fine-tuning, while *fine-tune* refers to one forward pass through the ICL-transformer after fine-tuning. Our work builds on TabPFN [20], so below we explain their dataset generator and their transformer architecture.

3.1 TabPFN Dataset Generator

The TabPFN authors create their own synthetic dataset using *Bayesian Neural Networks* (BNN) and *Structural Causal Models* (SCM). To construct a dataset, they first create a BNN or a SCM with random characteristics and with randomly initialized weights. Then they randomly draw an input \mathbf{X} and pass it through the model to generate output \mathbf{y} . Their final dataset is given by (\mathbf{X}, \mathbf{y}) . See their paper [20] for more details.

In their approach, they emphasize their ability to create realistic datasets, and even call their generator a "prior". They chose SCMs specifically because it can capture real-world causal mechanisms. One other aspect they focus on is simplicity, biasing the generator towards less complex input-output relationships. Additionally, they ensure the inputs \mathbf{X} have natural correlation by correlating the features blockwise, and they vary their feature importance by tuning the magnitude of weights belonging to different features. These methods suggest the authors believe creating realistic datasets is important for achieving good performance.

3.2 Architecture

In our work, we use the architecture from TabPFN, and make no changes to isolate the effect of the dataset generator. This ICL-transformer has as input the features $\mathbf{X}_{support} \in \mathbb{R}^{|S| \times d_f}$ and targets $\mathbf{y}_{support} \in \mathbb{N}^{|S|}$ from *support* set S and features $\mathbf{X}_{query} \in \mathbb{R}^{|Q| \times d_f}$ from *query* set Q . The output is a prediction for $\mathbf{y}_{query} \in \mathbb{R}^{|Q|}$. The query set Q represents the observations we want to predict, while the support set S are the observations we base our prediction on. This architecture accepts a fixed number of features d_f , see also the preprocessing discussed in Appendix A.3.

In this transformer, a token with dimension d_{token} represents all features of a single observation. The creation of support tokens $H_{support} \in \mathbb{R}^{|S| \times d_{token}}$ and query tokens $H_{query} \in \mathbb{R}^{|Q| \times d_{token}}$ are

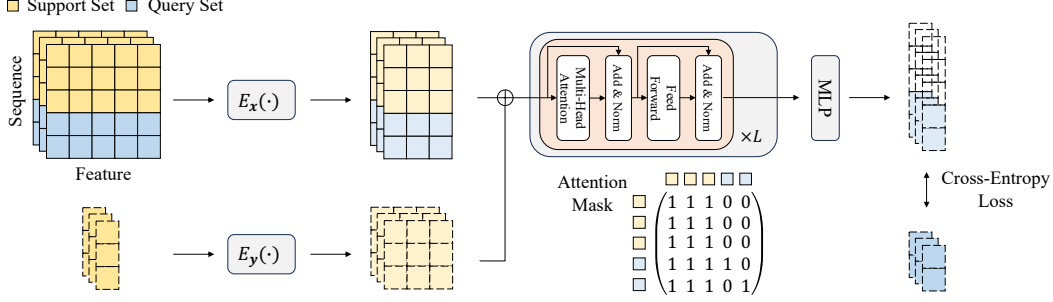


Figure 2: Base ICL-transformer architecture. On the left, dataset features and targets are separately encoded into tokens. On the right, the targets of the query dataset are used as label. In the middle is the ICL-transformer with the attention mask.

given by equations 1 and 2.

$$\mathbf{H}_{support} = \mathbf{X}_{support} \mathbf{W}_x + \mathbf{y}_{support} \mathbf{w}_y^T \quad (1)$$

$$\mathbf{H}_{query} = \mathbf{X}_{query} \mathbf{W}_x \quad (2)$$

Here, we embed the features linearly using weights $\mathbf{W}_x \in \mathbb{R}^{d_f \times d_{token}}$. Input classes $\mathbf{y}_{support}$ are also embedded using a linear layer with weights $\mathbf{w}_y \in \mathbb{R}^{d_{token}}$, in which $\mathbf{y}_{support}$ is treated as a float. Biases are used but omitted in the equations for conciseness. In Figure 2, E_x refers to the multiplication with \mathbf{W}_x and E_y represents the product with \mathbf{w}_y .

After the embedding, we push the tokens through a standard transformer architecture with a special attention mask. Support tokens are only able to see other support tokens, and query tokens can only see all support tokens and themselves, with no attention to other query tokens. This attention mask ensures the prediction of an observation does not depend on which other test observations are included in the forward pass. The complete architecture is given in Figure 2.

4 Methodology

The full tabular data classification pipeline is given by: synthetic data generation (3.1 and 4.1), data preprocessing (A.3), architectural design (3.2) and fine-tuning (4.2). In this section, we introduce our new dataset generator and our proposed fine-tuning procedure.

4.1 Forest Dataset Generation

Our goal is to create a simple dataset generator that generates datasets with complex patterns to train on, in contrast to the TabPFN [20] generator that aims to create realistic datasets. We base our generator on decision trees, because of their ability to create highly complex decision boundaries with minimal computation cost. The idea is to "overfit" the decision tree to randomly generated features and targets. This fitted decision tree is then used as a data-generating process. See Algorithm 1 for the method and Figure 3 for examples of generated data.

Algorithm 1 Forest Dataset Generation

Input: $n_classes, n_features, base_size, dataset_size, tree_depth, categorical_perc$
Draw $\mathbf{X} \sim \mathcal{N}(base_size, n_features)$
Draw $\mathbf{y} \sim \mathcal{N}(base_size)$
Fit a decision tree on (\mathbf{X}, \mathbf{y}) of depth $tree_depth$.
Draw $\mathbf{X}_2 \sim \mathcal{N}(dataset_size, n_features)$
Convert $categorical_perc$ features of \mathbf{X}_2 to categorical.
Predict \mathbf{y}_2 using the decision tree on \mathbf{X}_2 .
Transform \mathbf{y}_2 using quantile transformation to uniform.
Discretize \mathbf{y}_2 into $n_classes$ classes.
Output: $(\mathbf{X}_2, \mathbf{y}_2)$

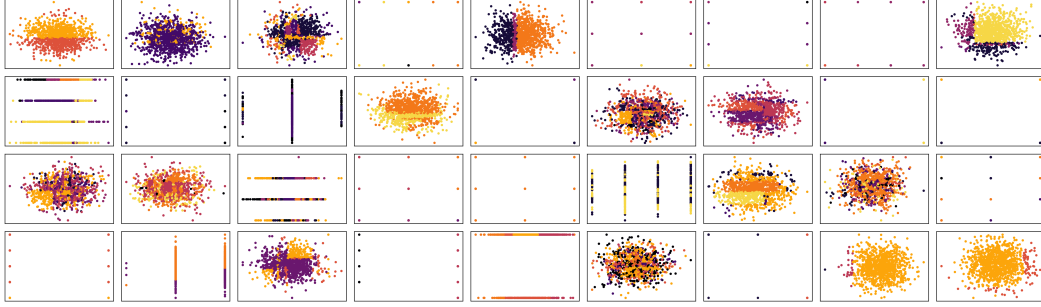


Figure 3: Generated forest data. Every box is a generated dataset with its own classes (color) and features (axes). The data clouds look unrealistic: decision boundaries are always orthogonal, and there is no feature correlation. Generated with base size 1024, dataset size 1024, maximum tree depth between 1 and 25, two features, and between 2 and 10 number of classes.

Our forest dataset generator allows datasets to vary in number of classes, observations, numerical features, and categorical features. There are two parameters that contribute to the decision boundary complexity. The *base size* is the number of observations used to fit the decision tree; more observations means more places for the decision tree to split on. The *tree depth* determines how deep the decision tree will go before exiting the fitting algorithm, with higher depth leading to greater complexity.

For every new synthetically generated dataset, we uniformly draw the hyperparameters from the bounds shown in Table 1. Because we have two hyperparameters that influence the complexity, we decided to keep the base size fixed. In the final step of the algorithm, the targets y_2 are discretized by uniformly drawing bucket boundaries between 0.0 and 1.0, and assigning a class to each bucket, creating varying degrees of class imbalance.

4.2 Fine-tuning Procedure

In our work, we introduce fine-tuning to the tabular ICL-transformer. When fine-tuning, we like to draw support and query sets from our training data such that the performance generalizes to the test set. This requires careful consideration of dataset splitting. The benchmark datasets already provide us with a training-validation-test split, of which the validation set is used for hyperparameter search. We require an additional validation set for early stopping, so we split the training with ratio 80/20 in training-small and validation-early-stopping.

Every gradient decent step, we randomly draw a 80/20 support and query split from training-small. For validation, we draw the support set from training-small, and draw the query set from validation-early-stopping. Every sample of the validation-early-stopping is seen exactly once, while support samples are randomly drawn with replacement. We use early stopping based on the validation loss, which is calculated after every step.

The early stopping technique can decide that training zero epochs is optimal, which allows us to fall back on the zero-shot performance in case fine-tuning harms the performance. This is especially important when using very small datasets. At the same time, fine-tuning can make use of the full training dataset, while the number of samples zero-shot can use is limited by the maximum support size that fits on the GPU.

5 Experiments

In our results we consider four pre-trained architectures, each with a zero-shot and a fine-tuned version:

Table 1: Hyperparameters for the Forest Dataset Generator

Hyperparameter	min	max
base size	1024	1024
dataset size	128	1024
tree depth	1	25
number of features	3	100
number of classes	2	10
ratio of categorical features	0.0	1.0

- **TabPFN (original)** is the original implementation by the TabPFN [20] authors, fine-tuned by us. The weights are downloaded from their Github.
- **TabPFN (retrained)** is trained by us on the TabPFN-dataset.
- **TabForest** is trained by us on our forest dataset.
- **TabForestPFN** is trained by us on both the TabPFN-dataset and our forest dataset.

Comparing the difference in behavior and performance allows us to learn the effect of the different synthetic datasets. Training and hyperparameter settings are given in appendix A.4, benchmarks used and results obtained are given below.

5.1 Introduction of the Benchmark Datasets

We show the results of our pre-trained architectures on two benchmarks, tested against publicly available results provided by the authors of the benchmarks. We include all their tested methods and datasets where possible. Appendix A.5 lists all used datasets.

The TabZilla [32] benchmark tests 20 algorithms on 176 classification datasets with sizes ranging from 32 observations to over a million. We selected 94 out of 176 datasets, see appendix A.5. The medium size benchmark which we refer to as WhyTrees [15] consists of 23 classification datasets with 2923 to a maximum of 10,000 observations.

Table 2: WhyTrees Results. Normalized accuracy for mixed and numerical features as shown in Figure 4.

	Mixed	Numerical
TabPFN (original) Zero-shot	0.530	0.587
TabPFN (original) Fine-tune	0.716	0.738
TabPFN (retrained) Zero-shot	0.207	0.351
TabPFN (retrained) Fine-tune	0.731	0.750
TabForest Zero-shot	0.208	0.350
TabForest Fine-tune	0.829	0.804
TabForestPFN Zero-shot	0.402	0.570
TabForestPFN Fine-tune	0.848	0.835

The benchmark is split into 7 datasets with only numerical features and 16 datasets with both numerical and categorical features.

Both benchmarks perform random hyperparameter search on their algorithms. TabZilla runs up to 30 times per algorithm and WhyTrees runs a few hundred times, up to 2500 runs. The ICL-transformers run only on default settings because we noticed little gains in performance when changing the fine-tuning hyperparameters.

5.2 Main Results of TabForestPFN

The results on the TabZilla benchmark are shown in Table 3, see Appendix A.6 for alternative presentations. For the WhyTrees benchmark, the comparison of fine-tuned TabForestPFN with the benchmark algorithm is shown in Figure 4, and the comparison with other ICL-transformer variants in Table 2.

In these figures and tables, we see that the fine-tuned TabForestPFN outperforms all other methods on TabZilla and matches the performance of XGBoost with a thousand runs on mixed features and a hundred runs on numerical features on WhyTrees. For both benchmarks, we can also see that there is a significant gap between the zero-shot performance of our retrained TabPFN and the original TabPFN. We attribute this phenomenon to the training settings, see Appendix A.4

Table 3: Main Results on TabZilla. N. Accuracy stands for Normalized accuracy. Rank compares the relative rank of a method compared to all other methods on that dataset. Only the 5 best methods out of 26 are shown. Full table with all methods is presented in Appendix A.6

Models	Rank				N. Accuracy	
	min	max	mean	median	mean	median
TabForestPFN - Fine-tune	1	24	8.0	6.0	0.680	0.663
TabPFN (retrained) - Fine-tune	1	26	8.3	7.8	0.678	0.700
CatBoost	1	22	8.9	7.8	0.676	0.663
XGBoost	1	23	9.2	8.2	0.674	0.671
TabPFN (original) - Fine-tune	1	25	9.3	8.0	0.670	0.677
⋮	⋮	⋮	⋮	⋮	⋮	⋮

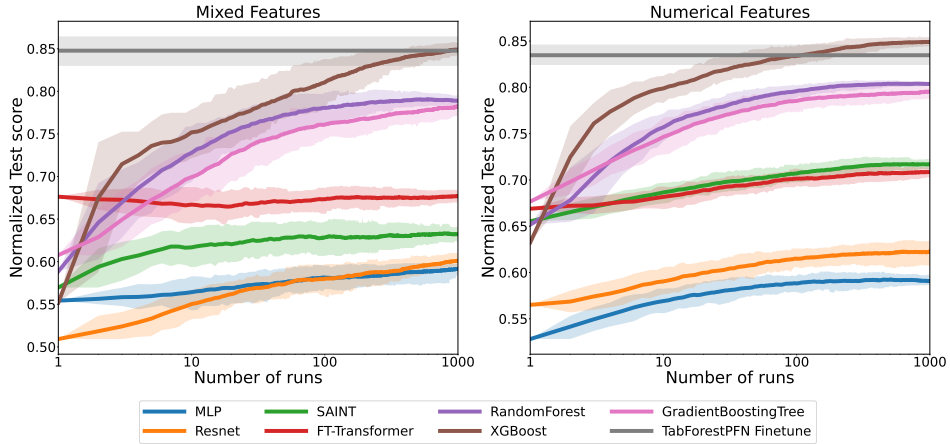


Figure 4: Main results on the WhyTrees Benchmark. TabForestPFN shows the mean over ten default runs for different fine-tuning seeds, all others use random search over the hyperparameters. See Table 2 for other ICL-transformers.

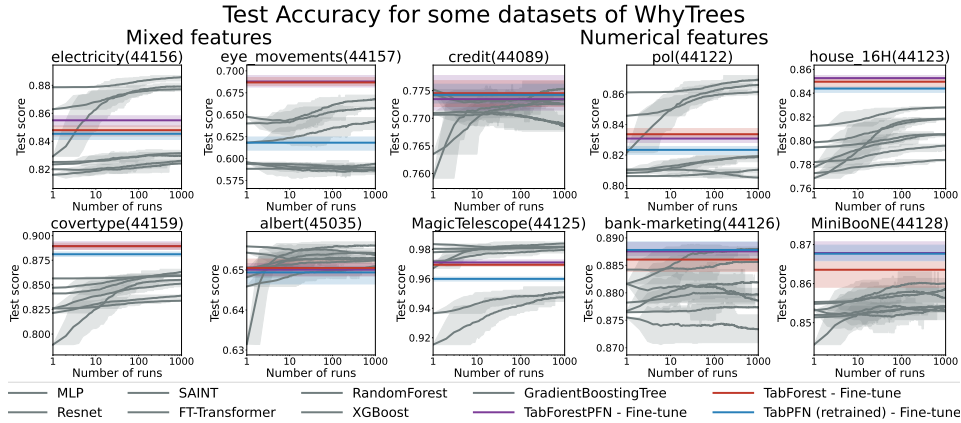


Figure 5: Comparison of TabForest, TabPFN and TabForestPFN on 10 datasets of the WhyTrees benchmark. Performance of different ICL-transformers is often similar. All the benchmark algorithms are greyed out. See Appendix A.7 for all WhyTrees datasets and for colored benchmark lines.

5.3 Similarity of TabPFN and TabForest

Now that we have established the strong performance of TabForestPFN, we take a closer look at the behavior of TabPFN versus TabForest. In Tables 4 and 6, we see that there is no clear favorite between the fine-tuned versions of TabPFN and TabForest: TabForest is the best on WhyTrees, while TabPFN is favored on TabZilla. Furthermore, TabForestPFN only has a marginal improvement over TabPFN on TabZilla, and similarly only a small performance increase over TabForest on WhyTrees.

In Figure 5 we show the performance of TabPFN, TabForest and TabForestPFN on individual datasets from the WhyTrees benchmark. Remarkably, all three methods often show similar performance across datasets, even though TabPFN and TabForest are pretrained on completely different synthetic data. These results suggest the TabPFN’s performance does not come from the fact that the synthetic dataset is a "prior". Instead the results suggest the performance is a property of an ICL-transformer’s learning process.

Furthermore, we see that there are some differences on some individual datasets, such as the *eye movements* and, to a lesser extent, the *bank-marketing* and *MiniBooNE* datasets. Although we cannot explain why these differences exist, it does prompt us to ensemble the synthetic datasets to create TabForestPFN, which seems to mimic the best method of the two.

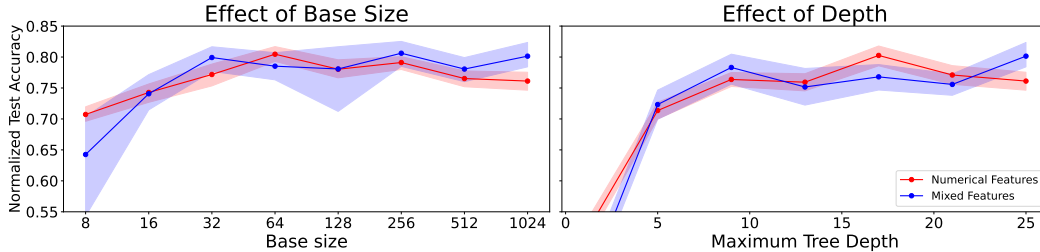


Figure 6: Ablation of the base size and maximum tree depth parameters of the Forest Dataset Generator. Figure shows normalized test accuracy of TabForest on the WhyTrees benchmark. A smaller model is used (dim: 512 -> 256, layers: 12 -> 8).

5.4 Complexity of ICL-Transformers’ Decision Boundaries

In the previous section, we have seen TabForest and TabPFN show similar performance behavior. Now we take a look at their decision boundaries. Repeating the analysis of the WhyTrees’ authors [15], we use Electricity dataset (OpenML ID: 44156) to predict a target on two features.

To capture the complexity of the decision boundary, we define the complexity score V . We split the feature space into a total of n grid cells where each cell has a predicted probability of class one p_{ij} for grid cell indices (i, j) . The complexity score V is defined as the sum of absolute values between neighbor cells:

$$V = \frac{1}{n} \sum_{ij} |p_{i+1,j} - p_{ij}| + |p_{i-1,j} - p_{ij}| + |p_{i,j+1} - p_{ij}| + |p_{i,j-1} - p_{ij}|$$

The complexity score represents how fast the prediction changes when moving along the grid.

We plot the results in Figure 1. We see that when fine-tuning, both TabPFN and TabForest can create decision boundaries that are more complex than regular MLPs. The complexity of the decision boundaries was one of the characteristics that explained why tree-based methods outperformed neural networks [15]. These results suggest ICL-transformers can also create complexity in the decision boundaries. In Appendix A.10 we also show that the complexity scales with the dimension of the ICL-transformer.

In our intuition, the ICL-transformer learns how to create these decision boundaries during pretraining. Different parameters of the network might be responsible for different parts of the decision boundary. During zero-shot, the ICL-transformer can then create the decision boundary out of these parts. During fine-tuning, the effect is stronger, as different parts come to the surface while irrelevant parts are tuned down.

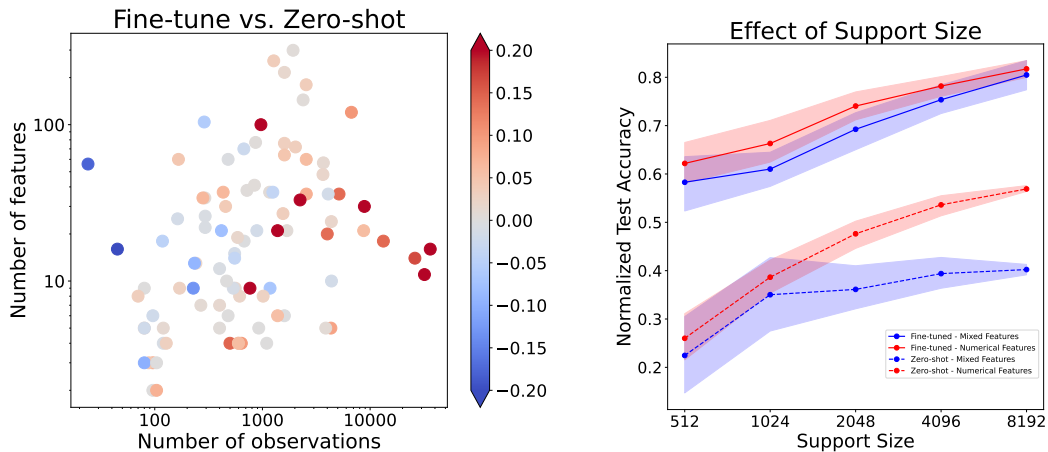
5.5 Ablation of the Forest Dataset Generator

In Section 4.1 we discussed two ways to influence the complexity of the forest dataset generator: the tree depth and the base size, which is the number of observations to fit the tree algorithm. We expect the performance of TabPFN to increase when the complexity of the forest dataset generator increases.

In Figure 6 we show the results of pretraining different settings of base size and maximum tree depth on the WhyTrees benchmark. The tree depth is set to 1-25 as the base size changes, and the base size is fixed to 1024 as the tree depth changes. When scaling up the base size from 8 to 32 and the tree depth from 1 to 9, we observe that the performance increases, and stabilizes for higher complexities. We provide figures of the data generated with these lower complexity hyperparameters in Appendix A.9 to give an impression. The correlation between performance and complexity supports our claim that learning complex decision boundaries is the driving force behind performance.

5.6 Superiority of Fine-tuning over Zero-shot

In the main results, we have seen that fine-tuning performs better than zero-shot. We look at this comparison in more detail. Figure 7a presents the performance of TabForestPFN on individual



(a) Differences in normalized accuracy of individual datasets from TabZilla. The color red means fine-tuning is the best. The darkest red represents at least 0.20 normalized score points improvement, and dark blue at least 0.20 normalized accuracy points degradation.

(b) Effect of different support sizes on the WhyTrees benchmark. Both fine-tuning and zero-shot performance improves with context size.

Figure 7: Evaluation of TabForestPFN

datasets from TabZilla. We can see clearly that fine-tuning strongly outperforms zero-shot when there are more than 10,000 observations. However, fine-tuning struggles on the two smallest datasets, which have four and six validation samples. Overall, fine-tuning outperforms zero-shot on 66% of the datasets. This percentage decreases to 54% for datasets smaller than a 1000 observations, and increases to 84% to datasets larger than a 1000 observations.

Figure 7b illustrates the effect of context length on the performance of TabForestPFN on the zero-shot and the fine-tuning task. We see that a higher support size is always better, which is why we set the support size in our paper to 8192, even though we only pretrained on a maximum size of 1024 observations. In conclusion, fine-tuning on the largest possible support size appears to be the most effective approach for ICL-transformers.

6 Conclusion

The introduction of TabPFN [20] has opened up a new field of *in-context learning* (ICL)-transformers for tabular data classification. Our research has demonstrated that these ICL-transformers learn to create complex decision boundaries. Furthermore, by fine-tuning and ensembling the pretraining dataset, we achieved performance levels that surpass XGBoost [6] and CatBoost [37] on third-party benchmarks [15, 32]. Although tree based-methods can continue to gain performance through hyperparameter optimization, we expect ICL-transformers can match their gains by scaling up the pretraining process.

Despite these advancements, there are still obstacles to overcome for ICL-transformers to fully replace tree-based methods in the realm of tabular data. One major challenge is the performance limitation of ICL-transformers due to GPU memory constraints. Our work uses fine-tuning as a solution to this problem, but it would be valuable to compare this approach to other concurrent research such as prompt tuning [11] and context distillation [30]. Moreover, our research solely focused on classification, although we expect a simple switch from cross-entropy loss to mean-squared-error loss would suffice to tackle regression tasks. Another area that requires exploration is the setting with an exceptionally high number of features [7], where the performance of ICL-transformers is unknown [31]. Lastly, tree-based methods have an edge in explaining the feature importance, and research needs to be done if ICL-transformers can achieve similar interpretability [40]. Overcoming these challenges will cement the ICL-transformer as the clear successor of tree-based methods.

References

- [1] Sercan Ö Arik and Tomas Pfister. Tabnet: Attentive interpretable tabular learning. In *Proceedings of the AAAI Conference on Artificial Intelligence*, volume 35, pages 6679–6687, 2021. Issue: 8.
- [2] Dara Bahri, Heinrich Jiang, Yi Tay, and Donald Metzler. SCARF: Self-Supervised Contrastive Learning using Random Feature Corruption. In *International Conference on Learning Representations (ICLR)*. arXiv, March 2022. doi: 10.48550/arXiv.2106.15147. URL <http://arxiv.org/abs/2106.15147>. arXiv:2106.15147 [cs].
- [3] Tom Brown, Benjamin Mann, Nick Ryder, Melanie Subbiah, Jared D Kaplan, Prafulla Dhariwal, Arvind Neelakantan, Pranav Shyam, Girish Sastry, Amanda Askell, Sandhini Agarwal, Ariel Herbert-Voss, Gretchen Krueger, Tom Henighan, Rewon Child, Aditya Ramesh, Daniel Ziegler, Jeffrey Wu, Clemens Winter, Chris Hesse, Mark Chen, Eric Sigler, Mateusz Litwin, Scott Gray, Benjamin Chess, Jack Clark, Christopher Berner, Sam McCandlish, Alec Radford, Ilya Sutskever, and Dario Amodei. Language Models are Few-Shot Learners. In *Advances in Neural Information Processing Systems (NeurIPS)*, volume 33, pages 1877–1901. Curran Associates, Inc., 2020. URL <https://proceedings.neurips.cc/paper/2020/hash/1457c0d6bfc4967418bfb8ac142f64a-Abstract.html>.
- [4] Kuan-Yu Chen, Ping-Han Chiang, Hsin-Rung Chou, Ting-Wei Chen, and Tien-Hao Chang. Trompt: Towards a Better Deep Neural Network for Tabular Data. In *International Conference on Machine Learning (ICML)*, May 2023. URL <https://openreview.net/forum?id=0yNmeyteuS>. arXiv:2305.18446 [cs].
- [5] Suiyao Chen, Jing Wu, Naira Hovakimyan, and Handong Yao. ReConTab: Regularized Contrastive Representation Learning for Tabular Data. In *NeurIPS Workshop: Table Representation Learning*, 2023.
- [6] Tianqi Chen and Carlos Guestrin. XGBoost: A Scalable Tree Boosting System. In *International Conference on Knowledge Discovery and Data Mining (KDD)*, pages 785–794, August 2016. doi: 10.1145/2939672.2939785. URL <http://arxiv.org/abs/1603.02754>. arXiv:1603.02754 [cs].
- [7] Valeriia Cherepanova, Roman Levin, Gowthami Somepalli, Jonas Geiping, C Bayan Bruss, Andrew Gordon Wilson, Tom Goldstein, and Micah Goldblum. A Performance-Driven Benchmark for Feature Selection in Tabular Deep Learning. In *Advances in Neural Information Processing Systems (NeurIPS)*, 2024.
- [8] Qingxiu Dong, Lei Li, Damai Dai, Ce Zheng, Zhiyong Wu, Baobao Chang, Xu Sun, Jingjing Xu, Lei Li, and Zhifang Sui. A Survey on In-context Learning, June 2023. URL <http://arxiv.org/abs/2301.00234>. arXiv:2301.00234 [cs].
- [9] Alexey Dosovitskiy, Lucas Beyer, Alexander Kolesnikov, Dirk Weissenborn, Xiaohua Zhai, Thomas Unterthiner, Mostafa Dehghani, Matthias Minderer, Georg Heigold, Sylvain Gelly, Jakob Uszkoreit, and Neil Houlsby. An Image is Worth 16x16 Words: Transformers for Image Recognition at Scale. In *International Conference on Learning Representations (ICLR)*. arXiv, June 2021. URL <http://arxiv.org/abs/2010.11929>. arXiv:2010.11929 [cs].
- [10] Benjamin Feuer, Niv Cohen, and Chinmay Hegde. Scaling TabPFN: Sketching and Feature Selection for Tabular Prior-Data Fitted Networks. October 2023. URL <https://openreview.net/forum?id=b00hN0ii36>.
- [11] Benjamin Feuer, Robin Tibor Schirrmeyer, Valeriia Cherepanova, Chinmay Hegde, Frank Hutter, Micah Goldblum, Niv Cohen, and Colin White. TuneTables: Context Optimization for Scalable Prior-Data Fitted Networks, March 2024. URL <http://arxiv.org/abs/2402.11137>. arXiv:2402.11137 [cs].
- [12] Yury Gorishniy, Ivan Rubachev, Valentin Khrulkov, and Artem Babenko. Revisiting Deep Learning Models for Tabular Data. In *Advances in Neural Information Processing Systems (NeurIPS)*. arXiv, 2021. URL <http://arxiv.org/abs/2106.11959>. arXiv:2106.11959 [cs] version: 3.
- [13] Yury Gorishniy, Ivan Rubachev, and Artem Babenko. On Embeddings for Numerical Features in Tabular Deep Learning. In *Advances in Neural Information Processing Systems (NeurIPS)*. arXiv, March 2022. URL <http://arxiv.org/abs/2203.05556>. arXiv:2203.05556 [cs].
- [14] Yury Gorishniy, Ivan Rubachev, Nikolay Kartashev, Daniil Shlenskii, Akim Kotelnikov, and Artem Babenko. TabR: Unlocking the Power of Retrieval-Augmented Tabular Deep Learning, July 2023. URL <http://arxiv.org/abs/2307.14338>. arXiv:2307.14338 [cs].
- [15] Léo Grinsztajn, Edouard Oyallon, and Gaël Varoquaux. Why do tree-based models still outperform deep learning on tabular data? In *Advances in Neural Information Processing Systems (NeurIPS)*. arXiv, July 2022. URL <http://arxiv.org/abs/2207.08815>. arXiv:2207.08815 [cs, stat].

- [16] Kaiming He, Xiangyu Zhang, Shaoqing Ren, and Jian Sun. Deep residual learning for image recognition. In *Proceedings of the IEEE conference on computer vision and pattern recognition*, pages 770–778, 2016.
- [17] M.A. Hearst, S.T. Dumais, E. Osuna, J. Platt, and B. Scholkopf. Support vector machines. *IEEE Intelligent Systems and their Applications*, 13(4):18–28, July 1998. ISSN 2374-9423. doi: 10.1109/5254.708428. URL <https://ieeexplore.ieee.org/document/708428>. Conference Name: IEEE Intelligent Systems and their Applications.
- [18] Stefan Hegselmann, Alejandro Buendia, Hunter Lang, Monica Agrawal, Xiaoyi Jiang, and David Sontag. TabLLM: Few-shot Classification of Tabular Data with Large Language Models. In *International Conference on Artificial Intelligence and Statistics (AISTATS)*, pages 5549–5581. PMLR, April 2023. URL <https://proceedings.mlr.press/v206/hegselmann23a.html>. ISSN: 2640-3498.
- [19] Jonathan Ho, Ajay Jain, and Pieter Abbeel. Denoising Diffusion Probabilistic Models. In *Advances in Neural Information Processing Systems (NeurIPS)*. arXiv, December 2020. URL <http://arxiv.org/abs/2006.11239>. arXiv:2006.11239 [cs, stat].
- [20] Noah Hollmann, Samuel Müller, Katharina Eggensperger, and Frank Hutter. TabPFN: A Transformer That Solves Small Tabular Classification Problems in a Second. In *International Conference on Learning Representations (ICLR)*. arXiv, September 2023. doi: 10.48550/arXiv.2207.01848. URL <http://arxiv.org/abs/2207.01848>. arXiv:2207.01848 [cs, stat].
- [21] Xin Huang, Ashish Khetan, Milan Cvitkovic, and Zohar Karnin. Tabtransformer: Tabular data modeling using contextual embeddings. *arXiv preprint arXiv:2012.06678*, 2020.
- [22] Arlind Kadra, Marius Lindauer, Frank Hutter, and Josif Grabocka. Well-tuned Simple Nets Excel on Tabular Datasets, November 2021. URL <http://arxiv.org/abs/2106.11189>. arXiv:2106.11189 [cs].
- [23] Liran Katzir, Gal Elidan, and Ran El-Yaniv. Net-DNF: Effective Deep Modeling of Tabular Data. In *International Conference on Learning Representations (ICLR)*, page 16, 2021.
- [24] Guolin Ke, Qi Meng, Thomas Finley, Taifeng Wang, Wei Chen, Weidong Ma, Qiwei Ye, and Tie-Yan Liu. LightGBM: A Highly Efficient Gradient Boosting Decision Tree. In *Advances in Neural Information Processing Systems*, volume 30. Curran Associates, Inc., 2017. URL <https://proceedings.neurips.cc/paper/2017/hash/6449f44a102fde848669bdd9eb6b76fa-Abstract.html>.
- [25] John A. Keith, Valentin Vassilev-Galindo, Bingqing Cheng, Stefan Chmiela, Michael Gastegger, Klaus-Robert Müller, and Alexandre Tkatchenko. Combining Machine Learning and Computational Chemistry for Predictive Insights Into Chemical Systems. *Chemical Reviews*, 121(16):9816–9872, August 2021. ISSN 0009-2665, 1520-6890. doi: 10.1021/acs.chemrev.1c00107. URL <https://pubs.acs.org/doi/10.1021/acs.chemrev.1c00107>.
- [26] Jannik Kossen, Neil Band, Clare Lyle, Aidan N Gomez, Thomas Rainforth, and Yarin Gal. Self-Attention Between Datapoints: Going Beyond Individual Input-Output Pairs in Deep Learning. In *Advances in Neural Information Processing Systems (NeurIPS)*, volume 34, pages 28742–28756. Curran Associates, Inc., 2021. URL <https://proceedings.neurips.cc/paper/2021/hash/f1507aba9fc82ffa7cc7373c58f8a613-Abstract.html>.
- [27] Roman Levin, Valeriia Cherepanova, Avi Schwarzschild, Arpit Bansal, C Bayan Bruss, Tom Goldstein, Andrew Gordon Wilson, and Micah Goldblum. TRANSFER LEARNING WITH DEEP TABULAR MODELS. In *International Conference on Learning Representations (ICLR)*, 2023.
- [28] Konstantinos G. Liakos, Patrizia Busato, Dimitrios Moshou, Simon Pearson, and Dionysis Bochtis. Machine Learning in Agriculture: A Review. *Sensors*, 18(8):2674, August 2018. ISSN 1424-8220. doi: 10.3390/s18082674. URL <https://www.mdpi.com/1424-8220/18/8/2674>. Number: 8 Publisher: Multidisciplinary Digital Publishing Institute.
- [29] Weizhang Liang, Suizhi Luo, Guoyan Zhao, and Hao Wu. Predicting Hard Rock Pillar Stability Using GBDT, XGBoost, and LightGBM Algorithms. *Mathematics*, 8(5):765, May 2020. ISSN 2227-7390. doi: 10.3390/math8050765. URL <https://www.mdpi.com/2227-7390/8/5/765>.
- [30] Junwei Ma, Valentin Thomas, Guangwei Yu, and Anthony Caterini. In-Context Data Distillation with TabPFN. In *NeurIPS Workshop: Table Representation Learning*. arXiv, 2023. doi: 10.48550/arXiv.2402.06971. URL <http://arxiv.org/abs/2402.06971>. arXiv:2402.06971 [cs] version: 1.
- [31] Calvin McCarter. What exactly has TabPFN learned to do?, 2024. URL <https://iclr-blogposts.github.io/2024/blog/what-exactly-has-tabpfn-learned-to-do/>.

- [32] Duncan McElfresh, Sujay Khandagale, Jonathan Valverde, Vishak Prasad C, Benjamin Feuer, Chinmay Hegde, Ganesh Ramakrishnan, Micah Goldblum, and Colin White. When Do Neural Nets Outperform Boosted Trees on Tabular Data? In *Advances in Neural Information Processing Systems (NeurIPS) Track on Datasets and Benchmarks*. arXiv, October 2023. URL <http://arxiv.org/abs/2305.02997>. arXiv:2305.02997 [cs, stat].
- [33] Jaehyun Nam, Jihoon Tack, Kyungmin Lee, Hankook Lee, and Jinwoo Shin. STUNT: Few-shot Tabular Learning with Self-generated Tasks from Unlabeled Tables. In *International Conference on Learning Representations (ICLR)*. arXiv, March 2023. URL <http://arxiv.org/abs/2303.00918>. arXiv:2303.00918 [cs].
- [34] Adeola Ogunleye and Qing-Guo Wang. XGBoost Model for Chronic Kidney Disease Diagnosis. *IEEE/ACM Transactions on Computational Biology and Bioinformatics*, 17(6):2131–2140, November 2020. ISSN 1545-5963, 1557-9964, 2374-0043. doi: 10.1109/TCBB.2019.2911071. URL <https://ieeexplore.ieee.org/document/8693581/>.
- [35] Guansong Pang, Chunhua Shen, Longbing Cao, and Anton Van Den Hengel. Deep Learning for Anomaly Detection: A Review. *ACM Computing Surveys*, 54(2):1–38, March 2022. ISSN 0360-0300, 1557-7341. doi: 10.1145/3439950. URL <https://dl.acm.org/doi/10.1145/3439950>.
- [36] Fabian Pedregosa, Gaël Varoquaux, Alexandre Gramfort, Vincent Michel, Bertrand Thirion, Olivier Grisel, Mathieu Blondel, Peter Prettenhofer, Ron Weiss, Vincent Dubourg, Jake Vanderplas, Alexandre Passos, David Cournapeau, Matthieu Brucher, Matthieu Perrot, and Édouard Duchesnay. Scikit-learn: Machine Learning in Python. *Journal of Machine Learning Research*, 12(85):2825–2830, 2011. ISSN 1533-7928. URL <http://jmlr.org/papers/v12/pedregosa11a.html>.
- [37] Liudmila Prokhorenkova, Gleb Gusev, Aleksandr Vorobev, Anna Veronika Dorogush, and Andrey Gulin. CatBoost: unbiased boosting with categorical features. In *Advances in Neural Information Processing Systems (NeurIPS)*. Curran Associates, Inc., 2018. URL <https://proceedings.neurips.cc/paper/2018/hash/14491b756b3a51daac41c24863285549-Abstract.html>. arXiv:1706.09516 [cs].
- [38] Matthew Richardson, Ewa Dominowska, and Robert Ragno. Predicting clicks: estimating the click-through rate for new ads. In *International Conference on World Wide Web (WWW)*, pages 521–530, Banff Alberta Canada, May 2007. ACM. ISBN 978-1-59593-654-7. doi: 10.1145/1242572.1242643. URL <https://dl.acm.org/doi/10.1145/1242572.1242643>.
- [39] Camilo Ruiz, Hongyu Ren, Kexin Huang, and Jure Leskovec. High dimensional, tabular deep learning with an auxiliary knowledge graph. In *Advances in Neural Information Processing Systems (NeurIPS)*, 2023.
- [40] David Rundel, Julius Kobialka, Constantin von Crailsheim, Matthias Feurer, Thomas Nagler, and David Rügamer. Interpretable Machine Learning for TabPFN, March 2024. URL <http://arxiv.org/abs/2403.10923>. arXiv:2403.10923 [cs, stat].
- [41] Harshay Shah, Kaustav Tamuly, Aditi Raghunathan, Prateek Jain, and Praneeth Netrapalli. The Pitfalls of Simplicity Bias in Neural Networks. In *Advances in Neural Information Processing Systems (NeurIPS)*, volume 33, pages 9573–9585. Curran Associates, Inc., 2020. URL <https://proceedings.neurips.cc/paper/2020/hash/6cfe0e6127fa25df2a0ef2ae1067d915-Abstract.html>.
- [42] Ira Shavitt and Eran Segal. Regularization Learning Networks: Deep Learning for Tabular Datasets. In *Advances in Neural Information Processing Systems (NeurIPS)*, volume 31. Curran Associates, Inc., 2018. URL <https://proceedings.neurips.cc/paper/2018/hash/500e75a036dc2d7d2fec5da1b71d36cc-Abstract.html>.
- [43] Ravid Shwartz-Ziv and Amitai Armon. Tabular data: Deep learning is not all you need. *Information Fusion*, 81:84–90, May 2022. ISSN 1566-2535. doi: 10.1016/j.inffus.2021.11.011. URL <https://www.sciencedirect.com/science/article/pii/S1566253521002360>.
- [44] Gowthami Somepalli, Micah Goldblum, Avi Schwarzschild, C. Bayan Bruss, and Tom Goldstein. SAINT: Improved Neural Networks for Tabular Data via Row Attention and Contrastive Pre-Training. In *NeurIPS Workshop: Table Representation Learning*. arXiv, June 2021. URL <http://arxiv.org/abs/2106.01342>. arXiv:2106.01342 [cs, stat].
- [45] Yi Sui, Tongzi Wu, Jesse C Cresswell, and Ga Wu. Self-supervised Representation Learning from Random Data Projectors. In *NeurIPS Workshop: Table Representation Learning*, 2023.

- [46] Talip Ucar, Ehsan Hajiramezanali, and Lindsay Edwards. SubTab: Subsetting Features of Tabular Data for Self-Supervised Representation Learning. In *Advances in Neural Information Processing Systems (NeurIPS)*, volume 34, pages 18853–18865. Curran Associates, Inc., 2021. URL <https://proceedings.neurips.cc/paper/2021/hash/9c8661befae6dbcd08304dbf4dcaf0db-Abstract.html>.
- [47] Joaquin Vanschoren, Jan N. Van Rijn, Bernd Bischl, and Luis Torgo. OpenML: networked science in machine learning. *ACM SIGKDD Explorations Newsletter*, 15(2):49–60, June 2014. ISSN 1931-0145, 1931-0153. doi: 10.1145/2641190.2641198. URL <https://dl.acm.org/doi/10.1145/2641190.2641198>.
- [48] Ashish Vaswani, Noam Shazeer, Niki Parmar, Jakob Uszkoreit, Llion Jones, Aidan N Gomez, Łukasz Kaiser, and Illia Polosukhin. Attention is All you Need. In *Advances in Neural Information Processing Systems (NeurIPS)*, volume 30. Curran Associates, Inc., 2017. URL <https://proceedings.neurips.cc/paper/2017/hash/3f5ee243547dee91fbd053c1c4a845aa-Abstract.html>.
- [49] Jinsung Yoon, Yao Zhang, James Jordon, and Mihaela van der Schaar. VIME: Extending the Success of Self- and Semi-supervised Learning to Tabular Domain. In *Advances in Neural Information Processing Systems (NeurIPS)*, volume 33, pages 11033–11043. Curran Associates, Inc., 2020. URL <https://proceedings.neurips.cc/paper/2020/hash/7d97667a3e056acab9aaf653807b4a03-Abstract.html>.
- [50] Guri Zabërgja, Arlind Kadra, and Josif Grabocka. Tabular Data: Is Attention All You Need? In *International Conference on Learning Representations (ICLR)*. arXiv, February 2024. URL <http://arxiv.org/abs/2402.03970>. arXiv:2402.03970 [cs].
- [51] Han Zhang, Xumeng Wen, Shun Zheng, Wei Xu, and Jiang Bian. Towards Foundation Models for Learning on Tabular Data, October 2023. URL <http://arxiv.org/abs/2310.07338>. arXiv:2310.07338 [cs].
- [52] Shuai Zhang, Lina Yao, Aixin Sun, and Yi Tay. Deep Learning Based Recommender System: A Survey and New Perspectives. *ACM Computing Surveys*, 52(1):1–38, January 2020. ISSN 0360-0300, 1557-7341. doi: 10.1145/3285029. URL <https://dl.acm.org/doi/10.1145/3285029>.
- [53] Qi-Le Zhou, Han-Jia Ye, Le-Ye Wang, and De-Chuan Zhan. Unlocking the Transferability of Tokens in Deep Models for Tabular Data. In *NeurIPS Workshop: Table Representation Learning*, 2023.
- [54] Bingzhao Zhu, Xingjian Shi, Nick Erickson, Mu Li, George Karypis, and Mahsa Shoaran. XTab: Cross-table Pretraining for Tabular Transformers. In *International Conference on Learning Representations (ICLR)*, June 2023. URL <https://openreview.net/forum?id=uGORNDmIdr>.

A Appendix

A.1 Ethics and Social Impact

Improving tabular data classification can provide major benefits to society. From medical to physics applications, better performance can save lives and money. There are, however, also more nefarious applications of tabular data classification, such as fraud risk detections based on ethnics or nationality; population analysis for micro-targeting political ad campaigns; and insurance premium discrimination based on underlying medical conditions.

Our models cannot detect the purpose for which the model is used. In contrast to large language models, our tabular data models take numerical data as input. Ethnicity, gender, or other sensitive information is represented by a class number. This means our models cannot recover the meaning behind the numbers.

A big benefit of this 'numerical anonymization' is privacy. In our paper, we use synthetic data, which is completely privacy risk free. But even when pretrained on real data, recovering the original data can be extremely hard due to the lack of labels and contextual information.

In light of the above, we decide to publish the model and open access to anyone. We do not know an effective way to create any form of safeguards against misuse, and we would welcome any advice from the research community that addresses this issue.

A.2 Code Availability

Code is available at <https://github.com/FelixdenBreejen/TabForestPFN>

The code includes everything: downloading datasets, preprocessing result benchmarks, training the ICL-transformers, pretrained weights on Google Drive, notebooks with analysis, and an easy example to get you started with applying the TabForestPFN to your dataset.

The code is built upon the works of Grinsztajn et al., Hollmann et al. and McElfresh et al.. Although this resulted in a Frankenstein monster of a codebase, we have made great efforts to rewrite most of their code to integrate well. The code assumes a single server with access to 1 or more GPUs, with DistributedDataParallel used during pretraining and multiprocessing over different GPUs used during inference.

As currently there is no good tabular code base out there, we recommend anyone that is interested in doing research in tabular data to take a look at ours.

A.3 Data Preprocessing

Before data is put into the neural network, the data is preprocessed. We use the exact same routine for both synthetic data and real-world data to ensure minimal differences in distribution and summary statistics of the input to the transformer. Algorithm 2 presents the procedure for preprocessing.

Algorithm 2 Data Preprocessing

Input: X_{raw}, y_{raw}

- 1: **Impute** NaN features with column mean.
- 2: **Remove** features with one unique value.
- 3: **Select** a subset of a hundred features.
- 4: **Transform** all features to normal using quantile transformation.
- 5: **Normalize** data to unit mean and variance.
- 6: **Scale** data based on number of features.
- 7: **Pad** the features to d_f features by adding zeros.
- 8: **if** Pretraining **then**
- 9: **Shuffle** the order of the features and classes.
- 10: **end if**

Output: $X_{preprocessed}, y_{preprocessed}$

Because we fixed the input size of the neural network to $d_f = 100$ features, we first select a subset of a d_f features using scikit-learn’s *SelectKBest* [36]. If there are less than d_f features, we add zeros to ensure exactly d_f features. Following TabPFN, we scale by multiplying by $100/d_{f*}$, where d_{f*} is the number of features after selecting a subset. To be robust to skewness and outliers, we transform the data using scikit-learn’s *QuantileTransformer* to follow a normal distribution. We make no distinction between numerical and categorical values in all our preprocessing.

In comparison to TabPFN, our data preprocessing follows roughly the same scheme. One change is the use of a quantile transformer, while they use standard input or a power transformer. We consider this a preference, both seem to work fine.

Furthermore, the TabPFN authors like to ensemble outputs of the TabPFN architecture, varying the transformation function between standard input and power transformer. In our paper, we use no ensembling at all.

A.4 Training Settings

All ICL-transformer architectures, including the original TabPFN, use the same model. The model consists of 12 layers, 4 attention heads, a hidden dimension of 512, and 10 classes as output dimension. Pretraining uses batch size 64, learning rate $1e-4$, weight decay 0.00, AdamW optimizer with betas (0.9, 0.95), cosine scheduling, and maximum global gradient norm 1.0. Fine-tuning is performed under batch size 1, learning rate $1e-5$, weight decay 0.00, no scheduling, with early stopping, and a maximum of 300 steps. To fit the model on an RTX 3090 with 24GB during fine-tuning, we set the maximum support size to 8192 samples and the maximum query size to 1024. Pre-training uses data generated with maximum support size 1024 and maximum query size 128. We choose these settings because the maximum support size affects performance, but the maximum query size only affects inference speed.

On these settings, we train TabPFN and TabForest for 300,000 steps, while TabForestPFN trains for 600,000 steps. Both TabPFN and TabForest can likely train longer; however, we experienced high instability in performance after 300,000 steps depending on the seed. Sometimes, the fine-tuning ability of the model would completely collapse, and sometimes the performance would slowly overfit. We also chose 300,000 steps because we did not see improvement in fine-tuning performance in the steps afterward. We chose to use 600,000 steps for the combined TabForestPFN, because we believed double the data would allow us to use double the steps, and we experienced no instability on this setting. Running 600,000 steps on one RTX 3090 takes 24 GPU-days.

Choosing 300,000 steps does have a downside. In the results in section 5.2, we saw the retrained TabPFN and the TabForest have poor zero-shot performance. The number of steps therefore is a trade-off: a small number of steps is stable and has high fine-tuning performance, while a large number of steps has good zero-shot performance. Because in this paper we are interested in maximum performance, we prioritize the fine-tuned version on 300,000 steps.

A.5 Benchmark Metadata

Of both the TabZilla and the WhyTrees benchmark, we show the OpenML[47] datasets we use as well as their characteristics. See Table 4 and Table 5. The TabZilla table presents the 94 datasets picked out of the 176 total datasets.

From the original 176 Tabzilla datasets, we excluded every dataset that does not have at least one completed run on default settings for every model, which brings the value to 99. Additionally, we exclude four datasets because they have more than 10 classes. The preprocessing code of one other dataset did not run without errors, and so is removed as well. The TabZilla authors did experiment with running TabPFN, but only on 62 datasets with a maximum support size of 3000 samples, so we redo their experiment.

Table 4: Metadata of the TabZilla Benchmark. Splits refers to the number of cross validation splits.

OpenML		Observations				Features	Splits	Classes
ID	Name	All	Train	Valid	Test			
3	kr-vs-kp	3196	2556	320	320	36	10	2

4	labor	57	45	6	6	16	10	2
9	autos	205	163	21	21	25	10	6
10	lymph	148	118	15	15	18	10	4
11	balance-scale	625	499	63	63	4	10	3
12	mfeat-factors	2000	1600	200	200	216	10	10
14	mfeat-fourier	2000	1600	200	200	76	10	10
15	breast-w	699	559	70	70	9	10	2
16	mfeat-karhunen	2000	1600	200	200	64	10	10
18	mfeat-morpholog...	2000	1600	200	200	6	10	10
23	cmc	1473	1177	148	148	9	10	3
25	colic	368	294	37	37	26	10	2
27	colic	368	294	37	37	22	10	2
29	credit-approval	690	552	69	69	15	10	2
30	page-blocks	5473	4377	548	548	10	10	5
35	dermatology	366	292	37	37	34	10	6
37	diabetes	768	614	77	77	8	10	2
39	sonar	208	166	21	21	60	10	2
40	glass	214	170	22	22	9	10	6
43	spambase	4601	3680	460	461	57	10	2
45	ssplice	3190	2552	319	319	60	10	3
47	tae	151	120	15	16	5	10	3
48	heart-c	303	241	31	31	13	10	2
49	tic-tac-toe	958	766	96	96	9	10	2
50	heart-h	294	234	30	30	13	10	2
53	vehicle	846	676	85	85	18	10	4
59	iris	150	120	15	15	4	10	3
2074	satimage	6430	5144	643	643	36	10	6
2079	eucalyptus	736	588	74	74	19	10	5
2867	anneal	898	718	90	90	38	10	5
3485	scene	2407	1925	241	241	299	10	2
3512	synthetic_contr...	600	480	60	60	60	10	6
3540	analcatdata_box...	120	96	12	12	3	10	2
3543	irish	500	400	50	50	5	10	2
3549	analcatdata_aut...	841	672	84	85	70	10	4
3560	analcatdata_dmf...	797	637	80	80	4	10	6
3561	profb	672	536	68	68	9	10	2
3602	visualizing_env...	111	88	11	12	3	10	2
3620	fri_c0_100_5	100	80	10	10	5	10	2
3647	rabe_266	120	96	12	12	2	10	2
3711	elevators	16599	13279	1660	1660	18	10	2
3731	visualizing_liv...	130	104	13	13	2	10	2
3739	analcatdata_chl...	100	80	10	10	3	10	2
3748	transplant	131	104	13	14	3	10	2
3779	fri_c3_100_5	100	80	10	10	5	10	2
3797	socmob	1156	924	116	116	5	10	2
3896	ada_agnostic	4562	3648	457	457	48	10	2
3902	pc4	1458	1166	146	146	37	10	2
3903	pc3	1563	1249	157	157	37	10	2
3904	jm1	10885	8707	1089	1089	21	10	2
3913	kc2	522	416	53	53	21	10	2
3917	kc1	2109	1687	211	211	21	10	2
3918	pc1	1109	887	111	111	21	10	2
3953	adult-census	32561	26048	3256	3257	14	10	2
9946	wdbc	569	455	57	57	30	10	2
9952	phoneme	5404	4322	541	541	5	10	2
9957	qsar-biodeg	1055	843	106	106	41	10	2
9960	wall-robot-navi...	5456	4364	546	546	24	10	4
9964	semeion	1593	1273	160	160	256	10	10
9971	ilpd	583	465	59	59	10	10	2
9978	ozone-level-8hr	2534	2026	254	254	72	10	2
9984	fertility	100	80	10	10	9	10	2
10089	acute-inflamat...	120	96	12	12	6	10	2
10093	banknote-authen...	1372	1096	138	138	4	10	2
10101	blood-transfusi...	748	598	75	75	4	10	2
14952	PhishingWebsite...	11055	8843	1106	1106	30	10	2

14954	cylinder-bands	540	432	54	54	37	10	2
14965	bank-marketing	45211	36168	4521	4522	16	10	2
14967	cjs	2796	2236	280	280	33	10	6
125920	dresses-sales	500	400	50	50	12	10	2
125921	LED-display-dom...	500	400	50	50	7	10	10
145793	yeast	1269	1015	127	127	8	10	4
145799	breast-cancer	286	228	29	29	9	10	2
145836	blood-transfusi...	748	598	75	75	4	10	2
145847	hill-valley	1212	968	122	122	100	10	2
145977	ecoli	336	268	34	34	7	10	8
145984	ionosphere	351	280	35	36	34	10	2
146024	lung-cancer	32	24	4	4	56	10	3
146063	hayes-roth	160	128	16	16	4	10	3
146065	monks-problems-...	601	480	60	61	6	10	2
146192	car-evaluation	1728	1382	173	173	21	10	4
146210	postoperative-p...	88	70	9	9	8	10	2
146607	SpeedDating	8378	6702	838	838	120	10	2
146800	MiceProtein	1080	864	108	108	77	10	8
146817	steel-plates-fa...	1941	1552	194	195	27	10	7
146818	Australian	690	552	69	69	14	10	2
146820	wilt	4839	3871	484	484	5	10	2
146821	car	1728	1382	173	173	6	10	4
167140	dna	3186	2548	319	319	180	10	3
167141	churn	5000	4000	500	500	20	10	2
167211	Satellite	5100	4080	510	510	36	10	2
168911	jasmine	2984	2386	299	299	144	10	2
190408	Click_predictio...	39948	31958	3995	3995	11	10	2
360948	libras	360	288	36	36	104	10	10

Table 5: Metadata of the WhyTrees Benchmark. Splits refers to the number of cross validation splits.

OpenML		Observations				Features	Splits	Classes
ID	Name	All	Train	Valid	Test			
44089	credit	16714	10000	2014	4700	10	2	2
44120	electricity	38474	10000	8542	19932	7	1	2
44121	covertype	566602	10000	50000	50000	10	1	2
44122	pol	10082	7057	907	2118	26	3	2
44123	house_16H	13488	9441	1214	2833	16	3	2
44125	MagicTelescope	13376	9363	1203	2810	10	3	2
44126	bank-marketing	10578	7404	952	2222	7	3	2
44128	MiniBooNE	72998	10000	18899	44099	50	1	2
44129	Higgs	940160	10000	50000	50000	24	1	2
44130	eye_movements	7608	5325	684	1599	20	3	2
44156	electricity	38474	10000	8542	19932	8	1	2
44157	eye_movements	7608	5325	684	1599	23	3	2
44159	covertype	423680	10000	50000	50000	54	1	2
45019	Bioresponse	3434	2403	309	722	419	5	2
45020	default-of-cred...	13272	9290	1194	2788	20	3	2
45021	jannis	57580	10000	14274	33306	54	1	2
45022	Diabetes130US	71090	10000	18327	42763	7	1	2
45026	heloc	10000	7000	900	2100	22	3	2
45028	california	20634	10000	3190	7444	8	1	2
45035	albert	58252	10000	14475	33777	31	1	2
45036	default-of-cred...	13272	9290	1194	2788	21	3	2
45038	road-safety	111762	10000	30528	50000	32	1	2
45039	compas-two-year...	4966	3476	447	1043	11	3	2

Table 6: Main Results on TabZilla. N. Accuracy stands for Normalized accuracy. Rank compares the relative rank of a method compared to all other methods on that dataset.

Models	Rank				N. Accuracy	
	min	max	mean	median	mean	median
TabForestPFN - Fine-tune	1	24	8.0	6.0	0.680	0.663
TabPFN (retrained) - Fine-tune	1	26	8.3	7.8	0.678	0.700
CatBoost	1	22	8.9	7.8	0.676	0.663
XGBoost	1	23	9.2	8.2	0.674	0.671
TabPFN (original) - Fine-tune	1	25	9.3	8.0	0.670	0.677
TabForestPFN - Zero-shot	1	26	10.6	10.0	0.633	0.650
TabForest - Fine-tune	1	24	10.6	9.5	0.650	0.667
TabPFN (original) - Zero-shot	1	25	10.9	10.2	0.632	0.606
LightGBM	1	26	11.1	11.0	0.646	0.653
RandomForest	1	25	11.3	11.0	0.636	0.637
Resnet	1	26	11.9	10.0	0.602	0.613
NODE	1	26	12.1	12.0	0.611	0.596
SAINT	1	26	12.2	12.8	0.600	0.614
SVM	1	25	12.5	13.2	0.589	0.573
FT-Transformer	1	23	12.6	12.5	0.599	0.601
DANet	3	25	14.5	15.0	0.596	0.608
MLP-rtdl	1	26	15.8	17.8	0.514	0.527
TabForest - Zero-shot	3	25	15.9	17.5	0.571	0.583
TabPFN (retrained) - Zero-shot	3	25	15.9	17.5	0.571	0.583
STG	1	26	16.1	17.2	0.495	0.472
LinearRegression	1	26	17.5	19.5	0.459	0.431
MLP	1	26	17.7	20.0	0.475	0.417
TabNet	2	26	18.0	19.0	0.503	0.490
DecisionTree	1	26	18.7	21.0	0.413	0.372
KNN	2	26	19.4	21.5	0.399	0.372
VIME	1	26	21.8	23.8	0.295	0.221

A.6 TabZilla Further Results

In the TabZilla main results Table 3, we have shown the five highest performing methods. The full results are shown in Table 6, which includes all ICL-transformer variants and methods implemented by the TabZilla authors. Because the rank is calculated over all included methods, which ICL-transformer variants we include might change the results. Therefore, we check if the results are the same if we use calculate the rankings one ICL-transformer at the time.

Table 7 shows the results of only the fine-tuned TabForestPFN versus the rest of the benchmark. We do this for every ICL-transformer and aggregate the results in Table 8. All results are qualitatively the same as in Table 3.

A.7 WhyTrees Further Results

The main results in Figure 4 report the normalized accuracy aggregated over all datasets. In Figure 8 we show the comparison between ICL-transformers on all 23 datasets. In Figure 9 we show the colored results on each individual dataset where we compare fine-tuned TabForestPFN with all the benchmark methods.

A.8 One-by-One Comparisons

In Figure 10 we plot one-to-one comparisons of fine-tuned TabForestPFN versus CatBoost, TabForest and TabPFN. We see no clear correlations in the other comparisons between performance difference and model.

Table 7: Main Results on TabZilla. N. Accuracy stands for Normalized accuracy. Rank compares the relative rank of a method compared to all other methods on that dataset.

Models	Rank				N. Accuracy	
	min	max	mean	median	mean	median
TabForestPFN - Fine-tune	1	18	5.8	4.2	0.680	0.663
CatBoost	1	15	6.2	5.2	0.676	0.663
XGBoost	1	16	6.3	5.0	0.674	0.671
LightGBM	1	19	7.6	6.0	0.646	0.653
RandomForest	1	18	7.9	8.0	0.636	0.637
NODE	1	19	8.4	8.0	0.611	0.596
Resnet	1	19	8.4	8.0	0.602	0.613
SAINT	1	19	8.5	7.2	0.600	0.614
SVM	1	18	8.6	8.0	0.589	0.573
FT-Transformer	1	16	8.8	8.5	0.599	0.601
DANet	2	19	10.0	10.0	0.596	0.608
MLP-rtdl	1	19	11.4	12.0	0.514	0.527
STG	1	19	11.5	12.0	0.495	0.472
LinearRegression	1	19	12.3	13.8	0.459	0.431
MLP	1	19	12.6	14.0	0.475	0.417
TabNet	1	19	12.8	13.8	0.503	0.490
DecisionTree	1	19	13.3	14.0	0.413	0.372
KNN	2	19	13.9	15.0	0.399	0.372
VIME	1	19	15.7	17.0	0.295	0.221

Table 8: Main Results on TabZilla. N. Accuracy stands for Normalized accuracy. Rank compares the relative rank of a method compared to all other methods on that dataset. This table displays individual results: Table 7 is run individually for all ICL-transformer variants, and the row of the ICL-transformer is copy-pasted here.

Models	Rank				N. Accuracy	
	min	max	mean	median	mean	median
TabPFN (original) - Zero-shot	1	19	7.4	6.0	0.632	0.606
TabPFN (original) - Fine-tune	1	19	6.4	5.0	0.670	0.677
TabPFN (retrained) - Zero-shot	2	19	10.7	11.8	0.571	0.583
TabPFN (retrained) - Fine-tune	1	19	5.9	5.0	0.678	0.700
TabForest - Zero-shot	2	19	10.7	11.8	0.571	0.583
TabForest - Fine-tune	1	19	7.4	7.0	0.650	0.667
TabForestPFN - Zero-shot	1	19	7.2	6.0	0.633	0.650
TabForestPFN - Fine-tune	1	18	5.8	4.2	0.680	0.663

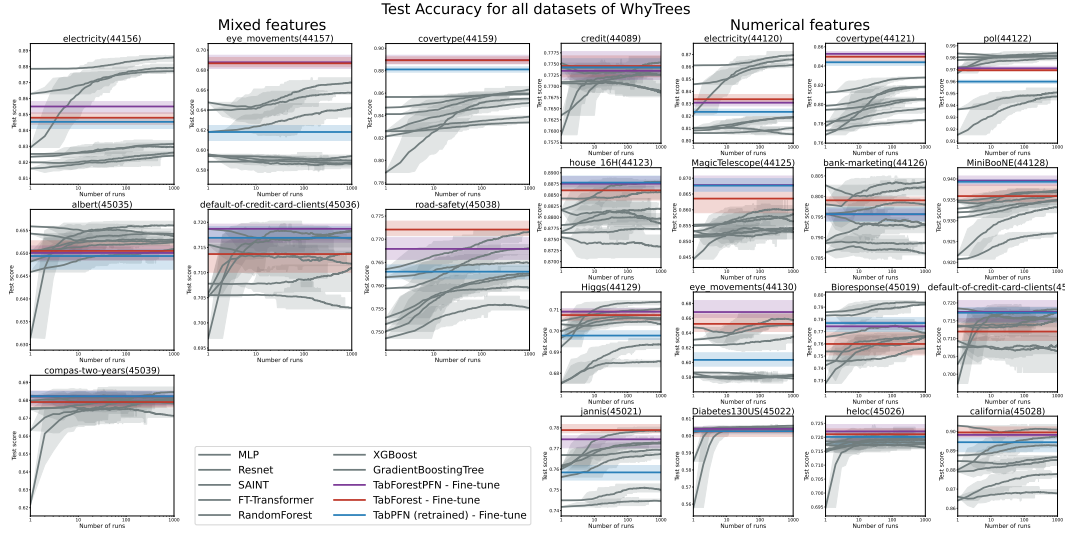


Figure 8: Comparison of TabForest, TabPFN and TabForestPFN on the WhyTrees benchmark. Performance of different ICL-transformers is often similar. All the benchmark algorithms are greyed out. See Appendix A.7 for colored benchmark lines.

S

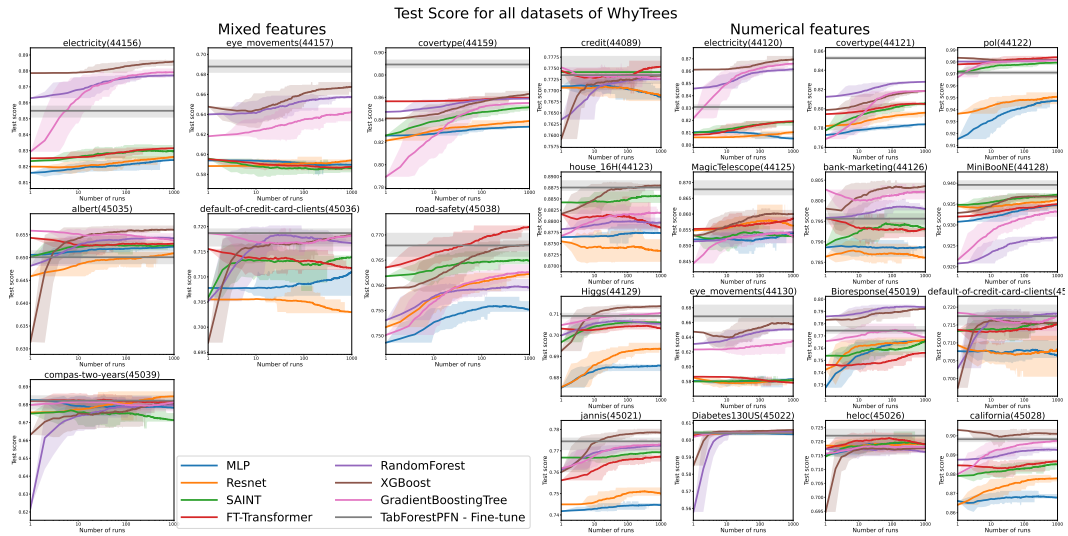


Figure 9: Individual dataset results on the WhyTrees Benchmark. TabForestPFN shows the mean of ten default runs, all others use random search over the hyperparameters. See Table 2 for other ICL-transformers.

A.9 Synthetic Data with Lower Complexity

In the ablation we have seen that even with a forest dataset generator with lower complexity parameters, we still have similar performance. To give an idea of how complex the data is, here we showcase the generated data. Figure 11 displays generated data with base size 32, and Figure 12 displays generated data with maximum tree depth 9.

A.10 Decision Boundaries for Scaled TabForest

In the complexity boundary results, we saw that TabForest has more complex decision boundaries when fine-tuned. Here we show that the complexity of the decision boundary is correlated with the

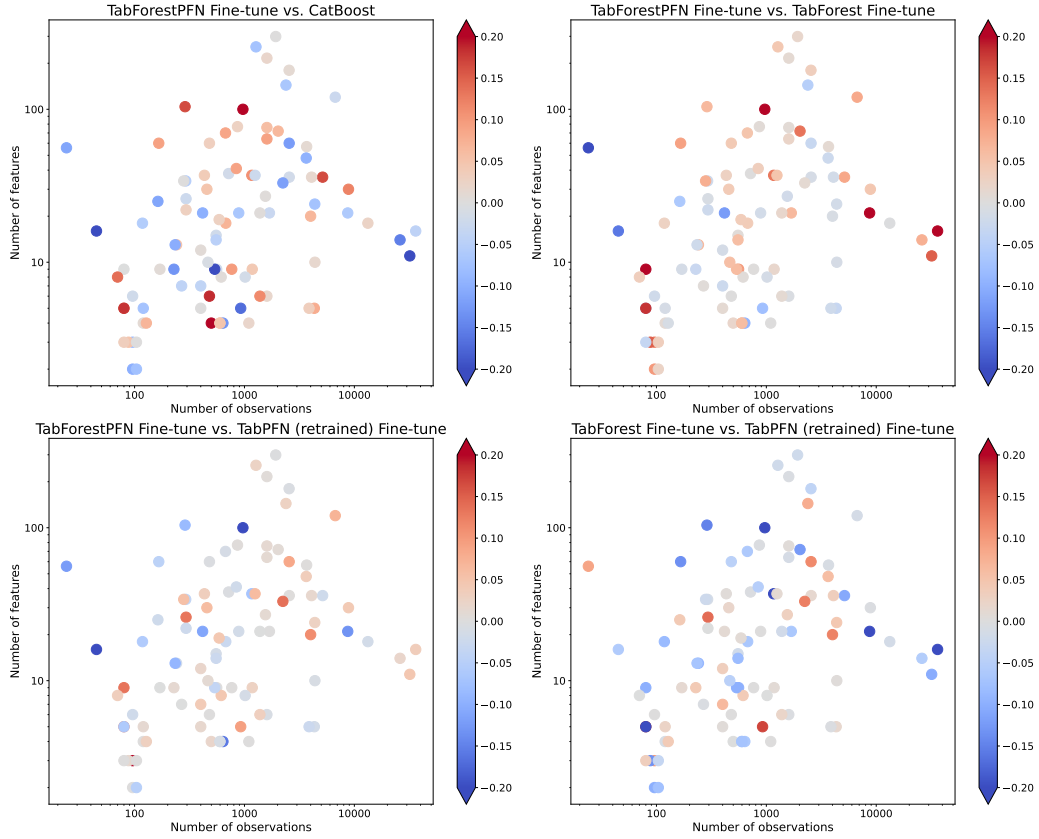


Figure 10: Differences in normalized accuracy of individual datasets from TabZilla. The color red means the left-mentioned method is the best, blue for the right-mentioned method. The darkest red represents at least 0.20 normalized score points improvement, and dark blue at least 0.20 normalized accuracy points degradation.

dimension size of the transformer. See Figure 13 for the results. We see that the decision boundaries become more complex when the dimension of the ICL-transformer increases.

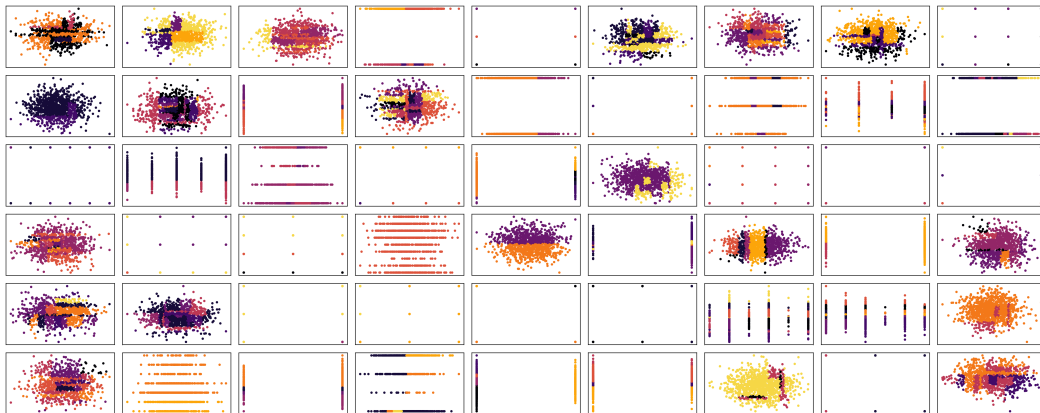


Figure 11: Generated forest data. Every box is a generated dataset with its own classes (color) and features (axes). Generated with base size 32, dataset size 1024, tree depth between 1 and 25, two features, and between 2 and 10 number of classes. See also Figures 3 and 12.

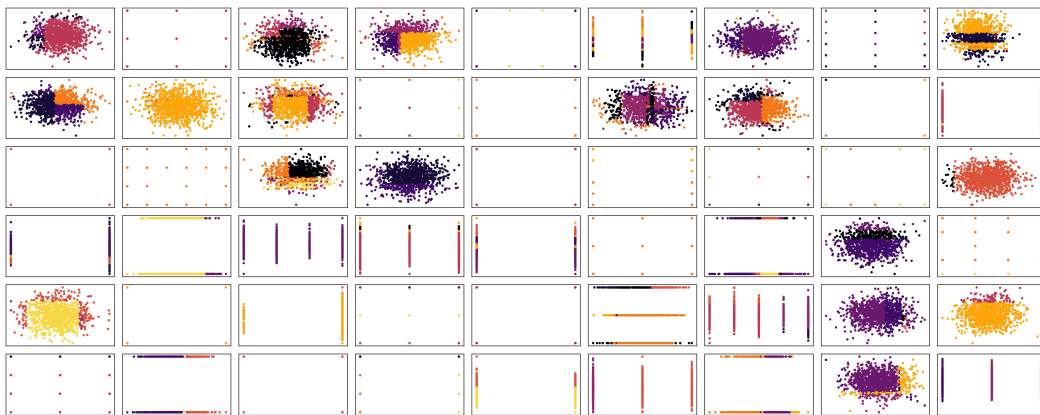


Figure 12: Generated forest data. Every box is a generated dataset with its own classes (color) and features (axes). Generated with base size 1024, dataset size 1024, tree depth between 1 and 9, two features, and between 2 and 10 number of classes. See also Figures 3 and 11.

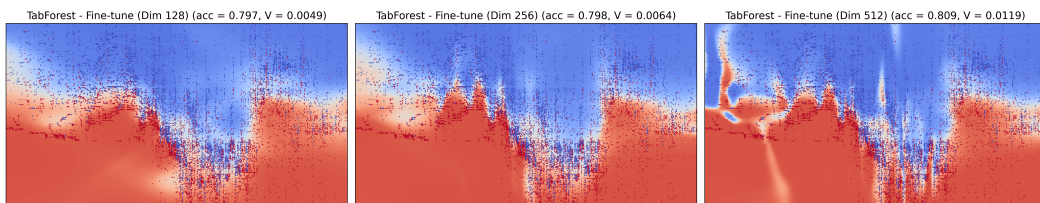


Figure 13: Comparison of decision boundaries for the electricity dataset. Axis represent features, color is predicted class probability, dots are test observations. When increasing the dimension size of the transformer, complexity increases.